Acoustic emission study on 50 years old reinforced concrete beams under bending and shear tests

Yang, Yuguang; Hordijk, Dick; de Boer, A.

Publication date
2016

Document Version
Accepted author manuscript

Published in
8th International Conference on Acoustic Emission

Acoustic emission study on 50 years old reinforced concrete beams under bending and shear tests

Yuguang Yang[1)], Dick A. Hordijk[1)], Ane de Boer[2)]

1) Delft University of Technology, Stevinweg 1, 2628 CN, Delft, the Netherlands.
2) Ministry of Infrastructure and the Environment, Griffioenlaan 2, 3526 LA, Utrecht, the Netherlands.

ABSTRACT: This paper presents the Acoustic Emission (AE) measurement of several tests carried out on reinforced concrete beams sawn from a 50 years old concrete bridge – Ruytenschildt bridge. The purpose of these tests is to provide additional information to the already executed in-situ load testing on the bridge. In addition to the AE measurement thorough crack width measurement was carried out during the tests. A strong correlation were obtained between the crack width and the AE measurements.

1 INTRODUCTION

The structural safety of the existing infrastructure has become an important issue in Europe in the last decade. The safety of the bridges and viaducts reduces due to the increase of the expected traffic load and degradation of their capacity. In the Netherlands, a large amount of concrete slab bridges are of concern. They were mostly constructed in the 50s or 60s without shear reinforcement. The aging process of the concrete influences their mechanical properties and cracks were generated. In addition, many of them have a different type of reinforcement (plain rebars with lower yielding strength) from what is commonly used nowadays. These aspects make an accurate theoretical evaluation of these existing concrete bridges rather difficult. An interesting alternative under development in Delft University of Technology in the Netherlands is the combination of proof loading (load testing) and Acoustic Emission (AE) measurement. In a proof loading, the bridge is loaded with a predefined loading condition to the target load level that is linked to certain structural safety level. Meanwhile the response of the bridge, including AE, is measured and compared with the expected structural response, which provides insight in the actual behaviour of the target structure. To achieve this, a thorough study of the acoustic emission signals of aged concrete is necessary.

In a proof loading, the test should not cause irreversible damage to the structure. For the development of the testing approach, it is rather important to understand the behaviour of such a structure at failure. For that reason, in 2014, a failure test was carried out on site on an existing concrete bridge (Ruytenschildt bridge) in the Netherlands [1]. The bridge was constructed in 1962, and was scheduled for demolition and replacement by a bridge with a larger clearance for ship traffic. It is a 5 span integral bridge. Two loading tests were carried out on two of the five spans of the bridge. Though shear failure was governing in the calculation, because of the rather low reinforcement ratio and the yielding strength of the tensile reinforcement, yielding of the tensile reinforcement was found in these tests. Acoustic Emission (AE) was measured during the tests as a pilot test to evaluate the damage that was caused at different stages of the loading program to provide additional information for the future non-destructive tests.

To obtain more information from this research, it was decided to saw three beams from the untested spans, and executed a few additional tests with different loading conditions in a more controlled way at Stevin laboratory of Delft University of Technology. In this paper, these additional beam tests and the AE measurement during the tests are presented. The AE measurement results are compared with the structural behaviour of the specimens, obtained from other measurements such as crack width. This served as complimentary information to the in situ bridge test.

2 TEST CONFIGURATIONS

This section provides a brief description of the beam test program. For more detailed information, the readers are referred to the test report [2].

2.1 *Test specimens*

The three beams from the Ruytenschildt bridge are numbered as RSB01 – RSB03. The length of the beams is 6 m. The intended width of the specimens was 500 mm for RSB01 and RSB02 and 1000 mm for RSB03. The coarse action of sawing resulted in a wider cross section than expected. The actual cross-sections of the specimens were measured at several different positions in the length direction, which resulted in the cross-sectional properties given in Table 1. For the bending tests, the dimensions of the critical section are taken, while for the shear tests, the average cross sectional properties are used.

The tensile reinforcement configurations of the specimens were determined based on the original drawing and visual inspection on the saw cut at the ends of the specimens. The reinforcement is plain rebars with mean yielding strength of f_{ym} = 283 MPa from lab tests. The reinforcement properties of the critical sections are given in Table 1 as well.

Table 1: Cross sectional propertied of the tested specimens

	RSB01F	**RSB02A**	**RSB02B**	**RSB03F**	**RSB03A**
***d* (mm)**	503	516	520	521	515
***w* (mm)**	577	576	590	1144	1043
A_c (m^2)	0.290	0.297	0.3066	0.596	0.537
Rebar	4Ø22+4Ø19	4Ø22+4Ø19	4Ø22+5Ø19	9Ø22+8Ø19	7Ø22+8Ø19
ρ_l	0.91%	0.89%	0.96%	0.95%	0.92%

Since the properties of the aged concrete was not known anymore, 62 concrete cylinders were drilled from the bridge prior to the in-situ tests to investigate the concrete strength [3]. Moreover, after the tests of the beams, additional cylinders were drilled from the undamaged part of the specimens. From these tests, the concrete strength was determined: f_{cm} = 52.2 MPa with COV = 17.3% [2]. Unlike a newly casted specimen, in the presented specimens, many cracks were observed. Accordingly, the global mechanical and wave transfer properties of the concrete of these specimens can not only be compared with the newly casted concrete with the same compressive strength.

2.2 *Test setup*

All the specimens were simply supported and were loaded by a single point load. The distance between the two supports is 5000 mm. The position of the point load varies according to the type of test. For the bending tests, the point load is located in the mid-point between the two supports. The corresponding tests are RSB01F and RSB03F. For shear test, the loading position is at 1250 mm from the support in tests RSB02A and RSB02B and 1300 in test RSB03A. Two examples of the test setup for flexural and shear tests are given in Figure 1.

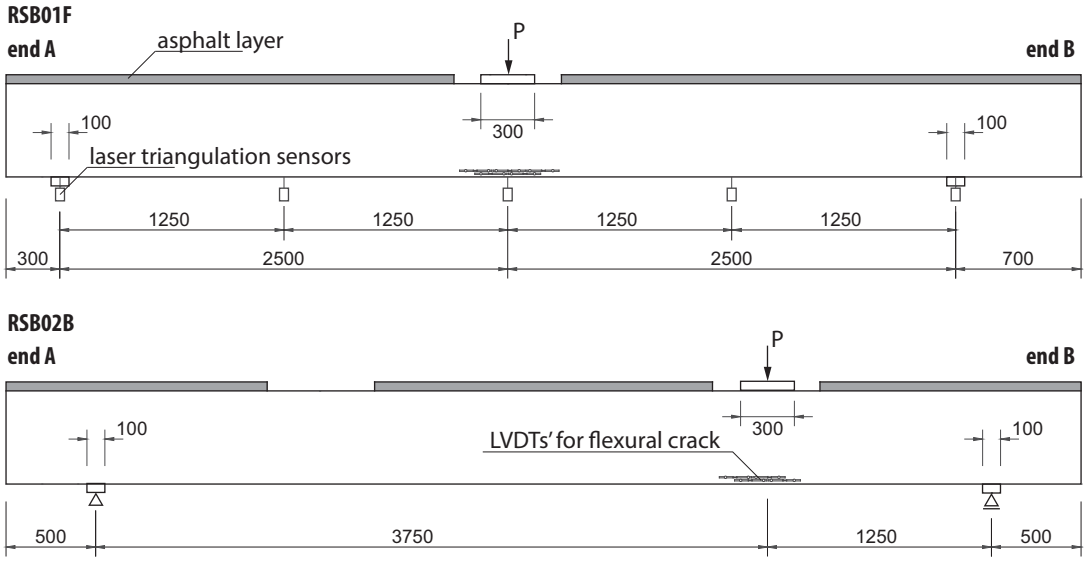

Figure 1: Configurations of the test setup for flexural tests (RSB01F) and shear tests (RSB02B), unit: mm.

The measurements during the test include the load level, the vertical deformation, the crack width and Acoustic Emission. An overview of the measurement equipment on the specimens is indicated in Figure 1. Amongst the others, the development of the first/maximum flexural crack width was measured by an array of LVDTs'. Figure 2 shows a photo of the LVDT array when the reinforcement yielded. The coverage of each LVDT overlaps with that of its neighbor, so that at least one of the LVDTs' is possible to capture the formation of the first flexural crack from the very beginning. Because of the loading condition of the test, one of the flexural cracks measured by the LVDT array will become the maximum flexural crack. In the later analysis, the measurement of this crack width is selected as the crack width under the loading point without further indication of the LVDT number.

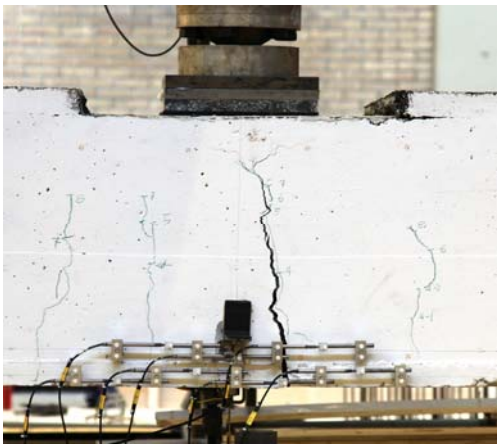

Figure 2: Layout of LVDTs' in test RSB01F after failure.

In addition to the traditional measurements, AE sensors were installed on the side surface and the bottom surface of the test specimens. The AE sensors that are used in the tests are R6I-AST. More information of the sensors is referred to [4]. Its response frequency is up to 100 kHz. During the test, the low frequency components (< 20 kHz) were filtered. As an example, the AE sensor layout of RSB03F is indicated in Figure 3. The layouts of each test varied slightly, for the AE sensor layouts of the other tests, the report [2] is referred to.

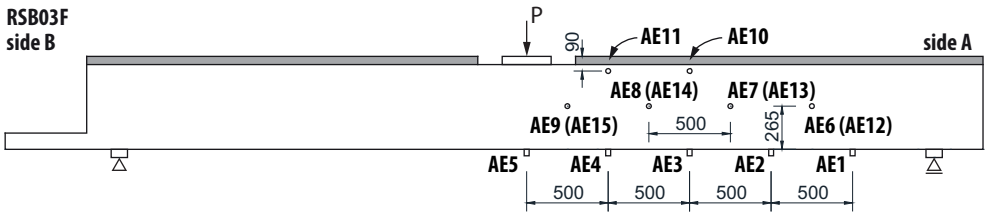

Figure 3: AE sensor layout for each test (sensor numbers in bracket were installed on the other side).

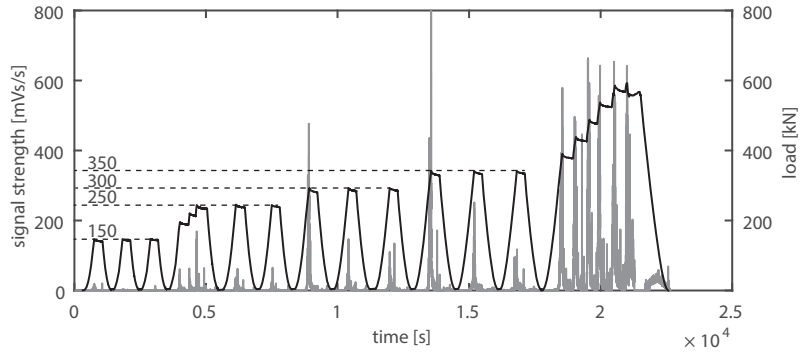

Figure 4: Loading history in comparison to the signal strength per second recorded by AE05 (under the point load) in tests RSB03F.

Cyclic loading was implemented in all the tests to determine the load ratio and calm ratio at different load levels. Several load steps were defined in the loading procedure. At each load step, three load cycles were planned.

An example of the loading procedure is given in Figure 4 in addition to the description of the loading procedures of the other tests in the test report [2].

3 STRUCTURAL BEHAVIOR

In all the tests, the specimens were loaded up to failure. In the two flexural tests, the tensile reinforcement yielded at failure. After the peak load, the load applied on the beams remained at a rather high level with an increasing irreversible deformation. While among the three shear tests, shear failure was obtained in test RSB02B and RSB03A, in which the specimen lost its capacity when an inclined flexural shear crack formed. A further discussion on these tests is given in [2]. While in RSB02A, despite the formation of an inclined crack, the maximum load was reached because of the yielding of the tensile reinforcement.

Despite the different failure modes, in this paper the main focus is on the relationship between the crack opening and the AE measurement. As discussed before, during a proof loading, the capacity of the tested structure is usually not reached. In that case, it is rather important to understand the distribution of the cracks and the opening of the cracks during the proof loading. In the presented tests, the specimens were loaded by a single point load, that results in a clear moment gradient along the span. Accordingly, the first flexural crack formed at the cross section under the loading position. The distribution of cracked sections spread further towards the supports with the increase of the load level. With the maximum flexural crack always located under the loading point. The maximum crack width – load relationships measured during the tests RSB01F and RSB03F are given in Figure 5. The sudden increase of crack width with respect to the load indicates the load level when the first flexural crack formed. In the case of RSB01F, the crack opening started when P_{cr} = 118.4 kN in the load step 100 kN – 125 kN, and continued in the step 125 kN – 150 kN. While in RSB03F, the cracking load was doubled, which is proportional to the width of the specimen.

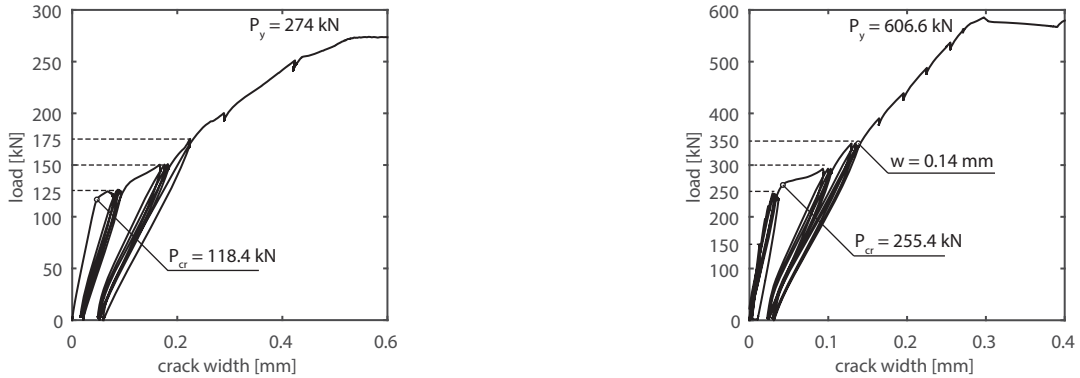

Figure 5: Crack opening - load relationship of Test RSB01F (left) and RSB03F (right).

4 AE MEASUREMENT

In the load testing of Ruytenschildt bridge, AE measurement was carried out. The intension was to use the load ratio and the calm ratio proposed by Ohtsu et al. in [5, 6] to indicate the cracking condition of the bridge at different load levels. However, because of the uncertainty of the mechanical and wave transfer properties of the concrete in the bridge, it was not clear how these values are related to the structural behavior of the bridge. It is expected that the measurements on the beam tests can provide additional information for the further assessment of the bridge test.

The load ratio and calm ratio were shown as one of the effective methods in the assessment of cracking behavior of structural concrete by tests on newly cased small scale reinforced concrete beams in [5, 7]. In this paper, signal strength is used instead of hits in the calculation of the load ratio and calm ratio calculation. With Cumulative Signal Strength (CSS), the measurement of a given AE sensor is less affected by the hits sourced from further away since the amplitude plays a role as well. In addition, with CSS the influence of the hits from cracking activities becomes more important compared to the other sources. The adjusted definition of load ratio and calm ratio are:

$$\text{load ratio} = \frac{\text{load at the onset of AE activity in the subsequent loading}}{\text{the previous maximum load}}$$

$$\text{calm ratio} = \frac{\text{the cumulative signal strength of AE activities during unloading}}{\text{the cumulative signal strength of AE activities during the whole cycle}}$$

In the loading test of Ruytenschildt bridge, only the bottom surface was accessible, therefore AE sensors were installed there. For calibration purpose, the sensors at the bottom surface in the beam tests are further evaluated. The load ratio and calm ratio of sensor AE01, AE03 and AE05 are given in Figure 6. The spacing of the three sensors is 1 m, which is the sensor distance applied in the in-situ test on Ruytenschildt bridge. In the load ratio calculation, the threshold was chosen to be 10 mVs, to exclude the irrelevant signals. If the CSS per second of a sensor did not reach the threshold throughout the whole cycle, the value of the load ratio was set as 1.0. In that case, although a calm ratio could still be calculated, the value should not be used for the structural assessment. Therefore, these data points are removed from Figure 6.

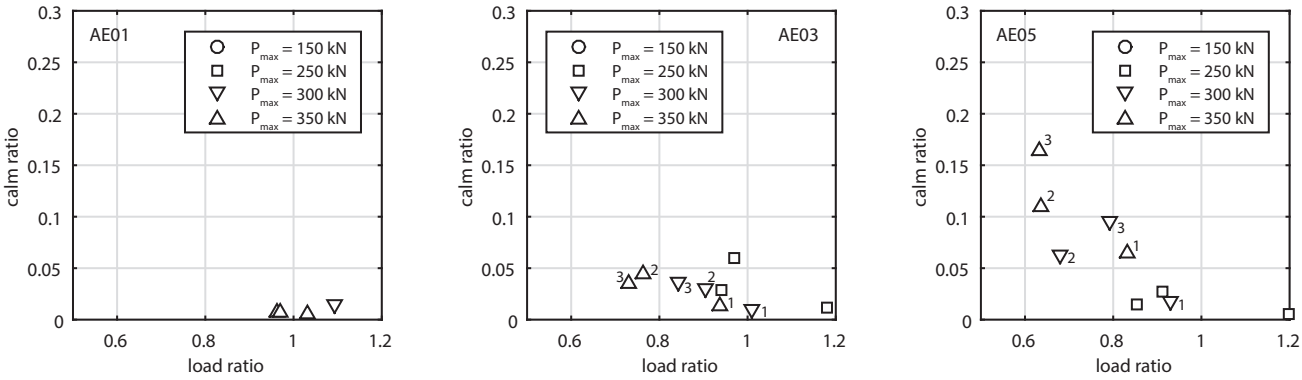

Figure 6. Calculated load and calm ratio (CSS based) of AE01 AE03 and AE05 in test RSB03F.

Taking into account the locations of the AE sensors, Figure 6 reflects properly the cracking of the specimen along the length direction. At the load step with P_{max} = 350 kN (last load step), the maximum crack width under the loading point was 0.14 mm according to Figure 5. A clearly higher calm ratio and lower load ratio is observed by AE05, which is located under the loading plate in the vicinity of the most flexural cracks according to Figure 3. AE03 shows very limited increase of calm ratio but considerable lower load ratio compare to AE01. According to the observation in the test, the last cracked section from the loading point at that load level was around AE04. The low load ratio and low calm ratio of AE03 suggests that the flexural cracks were developed, however, the crack width was quite limited. From the observation in Figure 6, it is also reasonable to assume that the calm ratio calculated by one AE sensor was not affected by the cracking activities from further away. This is because the amplitude of the hit generated during unloading is typically low.

When the calm ratio of AE03 and AE05 are compared, it turns out that the load ratio of AE05 was not significantly lower than AE03, but its calm ratio was much higher. Considering that the width of the cracks close to AE05 was wider than AE03, this observation suggests that the increase of the crack width is more related to the calm ratio, while the load ratio can be considered as an indication of the presence of the cracks. This observation confirms the assumptions given by Ohstu et al. based on hit rate in [5]. However, it has to be remarked that the repetition of the load cycles results a shift of both load ratios and calm ratios. In Figure 6, the load/calm ratios calculated in the 1st 2nd and 3rd cycles of the last load step was indicated. It shows that the calm ratio increases when the load cycle was repeated. The shift is because in the first load cycle, new cracks still has to be generated, thus the proportion of CSS in the whole cycle is less than the repeated cycles, see Figure 4. Since the CSS caused by cracking is related to the increase of the load level in the cycle, and the presence of existing cracks, it might be more robust to evaluate the calm ratios calculated from the repeated cycles.

To evaluate the effect of crack width and calm ratio, the relationship between the maximum crack width and the calm ratio calculated by AE sensors in the vicinity of the maximum flexural crack in test RSB01F, RSB03F and RSB02B are given in Figure 7. In all the three tests, the crack width and the calm ratio turns out to be strongly correlated. The comparison suggests that the calm ratio of the AE sensors can be used as an indication to the maximum crack width of the structure locally.

According to the definition, calm ratio reflects the AE activities during the unloading process. The specimens in this study are reinforced by plain bars, during the opening and closing of the crack, friction between rebar and concrete are expected. Since the crack width is the results of slip between concrete and the plain rebar, when the

friction of the interface is the source of AE activities during the unloading process, it is logical that the calm ratio is linearly related to the crack width. Though the calm ratio is affected by the repetition of the load cycles, Figure 7 shows that in the repeated cycles, this effect is less significant when the crack width is taken into account. Nevertheless, the dimensions of the cross section, the attenuation of the signal amplitude might affect the relationship between the calm ratio and crack width. Thus, further calibration is still needed to establish a solid relationship between calm ratio or CSS during unloading and the crack width.

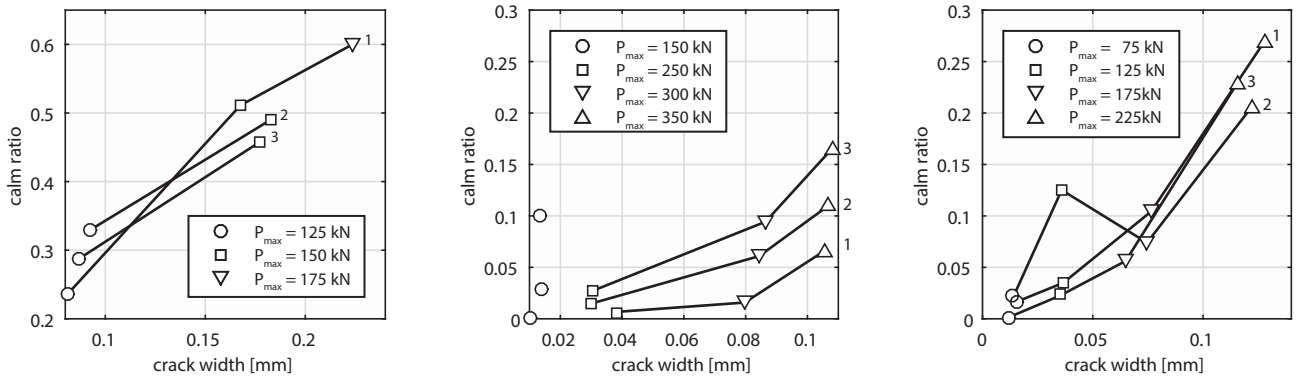

Figure 7: Relationship between calm ratio and crack width from left to right: RSB01F, RSB03F and RSB02B.

5 CONCLUSIONS

In this paper, the AE measurement during the tests on reinforced concrete beams sawn from an existing concrete bridge is reported. The tests provide a reference for the load ratio and calm ratio measured from the loading test on the Ruytenschildt bridge. The comparison between the calm ratio and the measured crack width suggests that the two parameters may be directly linked for such structures.

ACKNOWLEDGEMENTS

The authors would like to acknowledge the fanatical support of Technology Foundation STW and Rijkswaterstaat (Ministry of Infrastructure and the Environment of the Netherlands).

REFERENCES

[1] Lantsoght, E. O. L., van der Veen, C., de Boer, A. (2016) "Shear Capacity of the Ruytenschildt Bridge", *fib symposium*. Cape Town.

[2] Yang, Y., (2015) "Experimental Studies on the Structural Behaviours of Beams from Ruytenschildt Bridge", Stevin Report 25.5-15-09. Delft University of Technology: Delft. pp. 76.

[3] Wittenveen + Bos, (2015) "Materiaalonderzoek bruggen, zaaknummer 31084913, Brug over de Vierhuistervaart in de weg Heerenveen-Vierhuis (Ruytenschildbrug) aanvullingen 2015".

[4] Mistras, (2011) "Product data sheet of R6I-AST": http://www.physicalacoustics.com/by-product/sensors/R6I-AST-60-kHz-Integral-Preamp-AE-Sensor.

[5] Ohtsu, M., et al., (2002) "Damage assessment of reinforced concrete beams qualified by acoustic emission", *ACI Structural Journal*, 99(4): pp. 411-417.

[6] RILEM TC 212-ACD, (2010) "Recommendation of RILEM TC 212-ACD: acoustic emission and related NDE techniques for crack detection and damage evaluation in concrete", *Materials and Structures*, 43(9): pp. 1183-1186.

[7] Liu, Z.,Ziehl, P. H., (2009) "Evaluation of reinforced concrete beam specimens with acoustic emission and cyclic load test methods", *ACI Structural Journal*, 106(3): pp. 288-299.